2024 European Control Conference (ECC)
June 25-28, 2024. Stockholm, Sweden

Index Ratio Diagram – a new way to assess control performance

Paweł D. Domański

Abstract— **This paper presents a new way to conduct the control performance assessment (CPA). The measurement of control quality is a multi-criteria task from a practical point of view. Generally, the tuning of any controller means reaching a compromise between the accuracy and speed. The required (optimal) ratio between these two contradictory factors depends on the process demands, limitations and the engineering skills. Two basic indexes: the overshoot and settling time fit perfectly into such defined requirements. This research follows these path, but with the use of modern measures: robust statistical scale and shape factors, tail index and ARFIMA filter fractional order estimator. The assessment uses two dimensional Index Ratio Diagram (IRD), which allow to compare contradictory measures. Moreover, they allow to define new multi-criteria index able to compare different loops. The validation is compared against commonly used integral indicators.**

Index Terms— **control performance assessment, robust statistics, L-moments, tail index, ARFIMA, fractional order**

I. INTRODUCTION

Control performance assessment plays an important role in the engineering practice, as it supports a control engineer with a dedicated information about the loop performance. It's obvious why the CPA matters. Poor control worsens total process efficiency. Though this fact is not negotiable, there are quite a few control systems that are far away from being even close to the good operation. It's due to the insufficient daily care, process fluctuations, instrumentation breakdowns, wrong or outdated design, poor tuning, varying business requirements, lack of experienced staff, external impacts, uncertainties, human influence and many others [1]. Key performance indicators (KPIs) of control systems help an engineer to make a decision about control loop improvement. The CPA has to be used with clear and reliable methodology. The PID-based (Proportional-Integral-Derivative) single element loops form the overwhelming majority of control structures in process industry [2]. Thus, there are many dedicated approaches [3].

Reported CPA research started in 1967 [4] for pulp and paper plant utilizing statistical approach – process variable standard deviation. Since 1967 the CPA has explored many research areas [3], like the dedicated plant tests [5], model-based [6] or model-free [7] approaches. Single methodology algorithms are extended with hybrid techniques [8].

There is a general understanding that there is no single or universal method. Therefore, hybrid and multi-criteria approaches seem to give enough insight. Moment ratio diagrams (MRD) can be treated as such a tool [9]. L-moment ratio diagrams (LRMD) modify the MRDs giving scaled and robust approach [10]. This work takes the inspiration from the MRD and LMRD trying to explore their positives and fit them into control engineering. Generally, the system must meet some compromise between the speed and accuracy. Both demands cannot be fulfilled at the same time. This dilemma is clearly seen in the two basic measures of the system step response. The overshoot (κ) reflects control accuracy, while the settling time (T_{set}) informs about the speed. Though a solution to plot them in one diagram seems natural, it does not exist in the literature. Therefore, it is introduced and denoted as the Index Ratio Diagram – IRD(κ,T_{set}) [11].

The overshoot and settling time are derived using the loop step response, which is hardly achievable in practice. Apart from them, there are many other indexes that could replace them, like control error statistical scale factors and moments, integrals. Each of them has advantages and shortcuts, as they reflect different properties [3]. This article examines various variants of their use in the IRD framework. Additionally, a new control measure is brought into the picture and investigated – the tail index [12]. The use of tail index is justified by the fact that they allow to address the tails of the time series distributions and the industrial control errors are mostly heavy tailed [13].

The main contribution of this work is the introduction of the IRD diagrams into control engineering and multi-criteria performance assessment of the PID-based univariate loops. The secondary results lies in the incorporation of the tail index. The results are evaluated with the simulation environment, while the industrial aspects are shortly discussed. The paper starts with Section II describing methods followed by the simulation analysis included in Section III. Section IV concludes the paper disclosing observed open issues.

II. METHODS AND MEASURES

The research uses various statistical and CPA approaches, which are integrated within the proposed IRD framework analysis: basic integral measures [3], classical, robust and L-moments, accompanied with the tail index. The indexes are evaluated for the control error signal.

A. CPA integral indexes

The integral square error (ISE) is calculated as mean integral of the squared errors $\epsilon(k)$ over a set of discrete time moments $k = 1, \ldots, N$

$$\mathrm{ISE} = \frac{1}{N}\sum_{k=1}^{N}\epsilon^2(k). \tag{1}$$

[1]Paweł D. Domański is with Warsaw University of Technology, Institute of Control and Computation Engineering, ul. Nowowiejska 15/19, 00-665 Warsaw, Poland, pawel.domanski@pw.edu.pl

The ISE penalizes large observations neglecting the smaller ones. They usually appear after disturbances. It is seriously affected by outlying observations and is characterized with the 0% breakdown point [14]. The integral absolute error (IAE) sums error absolute values over time

$$\mathrm{IAE} = \frac{1}{N}\sum_{k=1}^{N} |\epsilon(k)| . \tag{2}$$

It is not so conservative as it penalizes continuing oscillations. Although its breakdown point is 0% as well, the IAE is robust against a part of outliers.

B. Statistical moments

One may use statistics in many ways. This paper follows a theoretical way assuming some distribution, which might reflect the underlying process. Such a probabilistic density function (PDF) we use to evaluate its factors and moments (if they exist). The other way is to approach the task empirically, when we need to estimate those parameters.

Let assume that $\{X_i\}^T$ represents a given time series with its mean μ and the *r*-th central moment $\gamma_r = E\left(X-\mu\right)^r$, $E\left(\cdot\right)$ is the expectation operator. The mean μ is the first moment γ_1, and variance σ^2 is the second one denoted as γ_2; σ is the standard deviation. These two moments are often used together with next ones: the skewness γ_3 and the kurtosis γ_4. The skewness presents data asymmetry and kurtosis the concentration.

$$\gamma_3 = \frac{1}{N\sigma^3}\sum_{i=1}^{N}\left(x_i - x_0\right)^3 \tag{3}$$

$$\gamma_4 = \frac{1}{N\sigma^4}\sum_{i=1}^{N}\left(x_i - x_0\right)^4 - 3 \tag{4}$$

The existence of outliers in data causes their distributions being fat tailed [15]. This feature biases classical estimation of the mean and standard deviation.

C. L-moments

The theory of L-moments has been proposed by Hosking [10] as a linear combinations of order statistics. The theory of L-moments includes new description of the PDF shape, helps to estimate factors of an assumed distribution and allows to test hypothesis about theoretical PDFs. We may define L-moments for any random variable, whose expected value exists. The L-moments give almost unbiased statistics, even for a small sample. They are less sensitive to the distribution tails [16]. This properties are appreciated in the life sciences, although they might be also used in control engineering. Their calculation is done as follows. The data $\{x_1, \ldots, x_N\}$, N - number of samples, are ranked in ascending order from 1 to N. Next, the sample L-moments $(l_1, \ldots, l_4)$, the sample L-skewness τ_3 and L-kurtosis τ_4 are evaluated as:

$$\begin{aligned} &l_1 = \beta_0,\ l_2 = 2\beta_1 - \beta_0,\ l_3 = 6\beta_2 - 6\beta_1 + \beta_0,\\ &l_4 = 20\beta_3 - 30\beta_2 + 12\beta_1 - \beta_0,\\ &\tau_2 = \frac{l_2}{l_1},\ \tau_3 = \frac{l_3}{l_2},\ \tau_4 = \frac{l_4}{l_2}, \end{aligned} \tag{5}$$

where

$$\beta_j = \frac{1}{N}\sum_{i=j+1}^{N} x_i \frac{(i-1)(i-2)\cdots(i-j)}{(N-1)(N-2)\cdots(N-j)} \tag{6}$$

Statistical properties are reflected in L-shift l_1, L-scale $l_2 \in\!< 0, 1)$, L-covariance (L-Cv) τ_2, L-skewness $\tau_3 \in (-1, 1)$ and L-kurtosis $\tau_4 \in (-1/4, 1)$. They help to fit a distribution to a dataset. L-skewness and L-kurtosis work as the goodness-of-fit measure. They can be calculated for theoretical PDFs [17] and normal distribution has: $l_1 = \mu$, $l_2 = \sigma/\pi$, $\tau_3 = l_3/l_2 = 0$ and $\tau_4 = l_4/l_2 = 0.1226$.

D. Robust statistics

One uses the robust statistics to address the issue of outliers. Robust estimators were introduced long ago, but works of Huber [18] discovered them for wider public. Robust methods allow to estimate the shift, the scale or regression parameters for data affected reach in outliers. This work uses the M-estimators with logistic psi-function implemented in the LIBRA toolbox [19].

E. Moment ratio diagrams

Moment ratio diagrams graphically show statistical properties of the considered time series in a plane The MRD is a graphical representation in a Cartesian coordinates of a pair of standardized moments. Actually, there are two versions [**?**]. The MRD(γ_3, γ_4) shows the third standardized moment γ_3 (or its square γ_3^2) as abscissa and the fourth moment γ_4 as ordinate, plotted upside down. There exists theoretical limitation of the accessible area, as $\gamma_4 - \gamma_3^2 - 1 \geq 0$. The locus corresponding to PDF can be a point, curve or region. It depends on the number of shape parameters. PDFs lacking shape factor (like Gauss or Laplace) are represented by a point, functions with one shape coefficient are represented by a curve. Regions reflect functions with two shape factors. The second type of the diagram MRD(γ_2, γ_3) represents variance γ_2 as the abscissa and skewness γ_3 as the ordinate. This diagram is location and scale dependent.

F. L-moment ratio diagrams

L-moments have been introduced by Hosking [10] and are common in the extreme analysis. They allow to identify proper distribution for empirical observations. The LMRD(τ_3, τ_4) shows the L-kurtosis τ_4 versus L-skewness τ_3 and the LMRD(l_2, τ_3) relates the skewness to the scale factor (L-l2 variance).

G. The α-stable distribution

Apart from the specific robust estimators or L-moments one may use other distributions. Stable functions deliver an alternative set of the statistical measures [3]. The α-stable distribution is expressed by the characteristics equation

$$F^{\mathrm{stab}}_{\alpha,\beta,\delta,\gamma}\left(x\right) = \exp\left\{i\delta x - \left|\gamma x\right|^{\alpha}\left(1 - i\beta l\left(x\right)\right)\right\}, \tag{7}$$

where

$$l\left(x\right) = \begin{cases} \mathrm{sgn}\left(x\right)\tan\left(\frac{\pi\alpha}{2}\right) & \text{for } \alpha \neq 1 \\ \mathrm{sgn}\left(x\right)\frac{2}{\pi}\ln\left|x\right| & \text{for } \alpha = 1 \end{cases} \tag{8}$$

The coefficient $0 < \alpha \leq 2$ is called the stability index, the $|\beta| \leq 1$ is the skewness factor, $\delta \in \mathbb{R}$ the shift and $\gamma > 0$ the scale. Thus, the α-stable distribution has one shift factor, one scale and two shape coefficients: α and β.

H. Tail index

Statistics frequently use the law of large numbers and the central limit theorem. Once data exhibits outliers, which is revealed in the form of tails, the majority of the assumptions made are not met. In such a case the knowledge, where the tail starts, and which observations are located in the tail plays an important role [21], [22]. There are many methods to estimate it and the tail index, denoted as $\hat{\xi}$, is the most promising one [23]. There are quite a few tail index estimation approaches, with two leading ones: the Hill [24] and Huisman estimator [25]. This research uses the second one in the analysis.

III. SIMULATION ANALYSIS

Dedicated Matlab environment is prepared with the PID controller in a parallel form. The analysis focuses on univariate PID control with three processes, proposed by Åström [26] as control benchmarks:

– System with Multiple Equal Poles

$$G_1(s) = \frac{1}{(s+1)^4}, \tag{9}$$

– First Order System with Dead Time

$$G_4(s) = \frac{1}{(0.2s+1)^2} e^{-s}, \tag{10}$$

– Fast and Slow Modes

$$G_5(s) = \frac{1}{(s+1)(0.04s^2+0.04s+1)}. \tag{11}$$

These transfer functions allow to consider relatively wide scope of processes. All simulated models are discretized with a sampling period $T_p = 0.1$ [s]. Setpoint is constant and set to zero. Loops are disturbed by:

- simulated Gaussian $N(0, \sigma^2)$ measurement noise with standard deviation $\sigma = 0.1 \cdot \sqrt{2}$,
- and filtered (first order filter) fat-tail disturbance added before the process and simulated using α-stable distribution with $\alpha = 1.95$, $\gamma = 2.0$ and $\beta = \delta = 0$.

The detailed analysis procedure is presented for the first process $G_1(s)$, while the following two are used to confirm and visualized obtained results. Fig. 1 shows exemplary time trend of the $G_1(s)$ controlled by the well-tuned PID controller $k_p = 1.0503$, $T_i = 2.9977$, $T_d = 0.9293$. The good controller for the $G_4(s)$ has $k_p = 0.2653$, $T_i = 0.6066$, $T_d = 0.2121$, and for the $G_5(s)$: $k_p = 0.1330$, $T_i = 0.2585$, $T_d = 0.0808$.

The analysis uses various PID parameter sets. The gain $k_p \in \langle 0.05; 2.05 \rangle$ changes every 0.25, the integration time $T_i \in \langle 0.2; 10.2 \rangle$ changes every 1.0 and the derivative is constant $T_d = 0.9293$. To exclude the statistical effects, each set of parameters is run 50 times and the resulting CPA measures are averaged. The same approach is repeated for other two

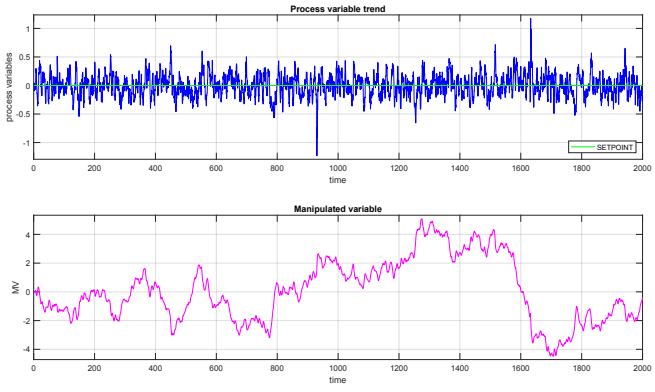

Fig. 1: Time series for loop $G_1(s)$ and well-tuned PID tuning

transfer functions. For the $G_4(s)$ the $k_p \in \langle 0.2; 1.6 \rangle$ changes every 0.2, the integration time $T_i \in \langle 0.1; 5.1 \rangle$ changes every 0.5 and the derivative is constant $T_d = 0.2121$. For the $G_5(s)$ the $k_p \in \langle 0.02; 1.02 \rangle$ changes every 0.1, the integration time $T_i \in \langle 0.05; 2.3 \rangle$ changes every 0.25 and the derivative is constant $T_d = 0.0808$.

The loop performance analysis starts with the IRD(κ,T_{set}) diagram sketched in Fig. 2, which compares the overshoot against the settling time. We clearly see a kind of the Pareto-front of the best solutions according to different preferences. The diagram is shaded according to the IAE index, because we always miss one indicator. Generally, such a drawing delivers only some relative visual information - we still would like to have a single loop performance indicator. Actually, an engineer could select that the best tuning is reflected by the shortest distance from the origin point $[x_0; y_0] = [0; 0]$. Moreover, one would wish to have this value independent on the real units of time and overshoot. Thus, we scale it and obtain the following IRD distance index $d_{IRD(x,y)}$ for scaled values x and y:

$$d_{IRD(x,y)} = \frac{1}{\sqrt{2}} \sqrt{(x-x_0)^2 + (y-y_0)^2} \tag{12}$$

The next Fig. 3 shows the scaled plot with scaling factors $x_{max} = 80$ and $y_{max} = 500$. The diagram indicates the best tuning depicted as the yellow square. This best PID controller obtains $d_{IRD(\kappa,T_{set})} = 0.013$ for the following parameters: $k_p = 0.55$ and $T_i = 3.20$. The pink square indicates the preselected well-tuned PID loop.

As the overshoot and settling time are hardly achievable in practice, other indicators should be brought to the picture. We suggest to use other measure, which can be evaluated with the operation control error data. Moreover, they should somehow reflect the time and the accuracy. We propose to use some variability measure and distribution shape factor.

Let's investigate robust standard deviation σ_R and the tail index $\hat{\xi}$. Fig. 4 shows the IRD(σ_R,$\hat{\xi}$) diagram related to the IAE, while Fig. 5 shows the same plot related to the ISE index. Scaling factors are $x_{max} = 1.5$ and $y_{max} = 15$

Now, the best PID controller obtains $d_{IRD(\sigma_R,\hat{\xi})} = 0.270$ for the following parameters: $k_p = 0.05$ and $T_i = 6.20$. There is also visible difference between the IAE and ISE.

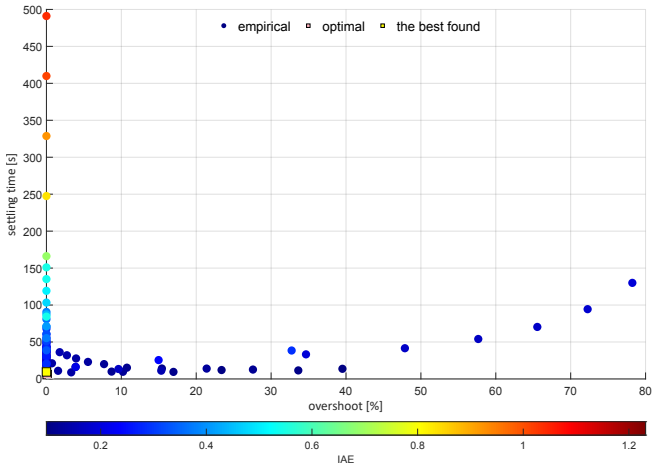

Fig. 2: IRD(κ,T_{set}) diagram for $G_1(s)$: pink square depicts good tuning, while yellow – the best found (the circles are shaded according to the IAE value) (points overlap each other)

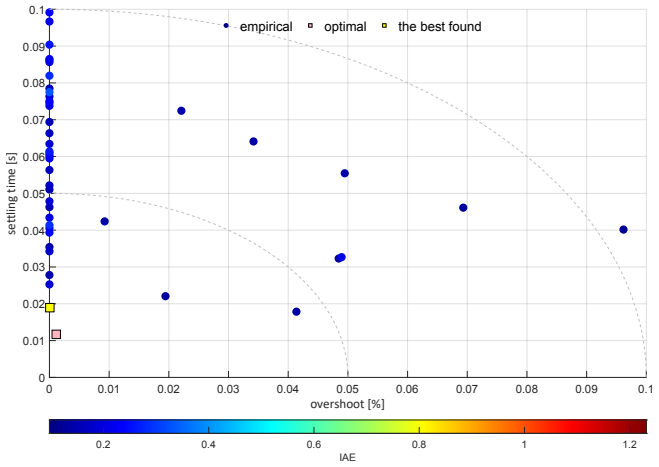

Fig. 3: Scaled IRD(κ,T_{set}) diagram for $G_1(s)$

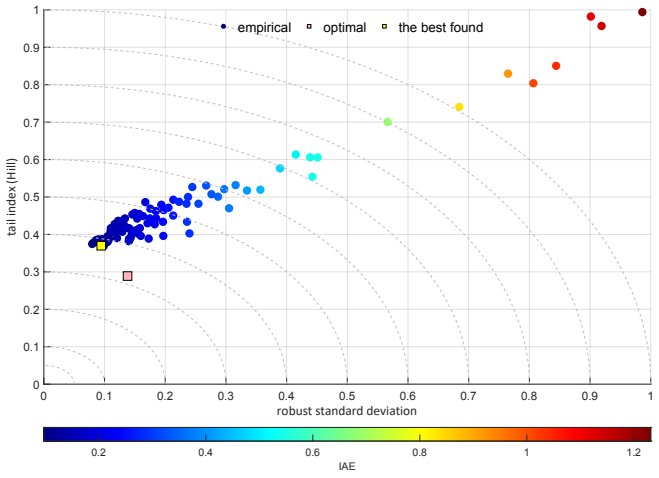

Fig. 4: IRD(σ_R,$\hat{\xi}$) diagram for $G_1(s)$: pink square depicts good tuning, while yellow – the best found (the circles are shaded according to the IAE value)

We clearly see that ISE starts to differentiate between tuning for worse controllers, than the IAE.

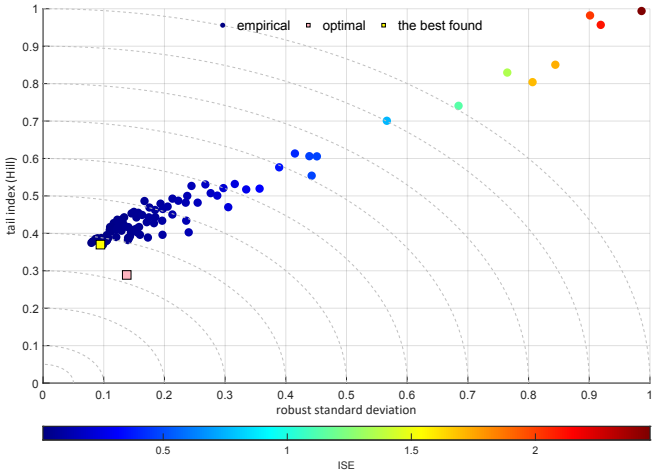

Fig. 5: IRD(σ_R,$\hat{\xi}$) diagram for $G_1(s)$: pink square depicts good tuning, while yellow – the best found (the circles are shaded according to the ISE value)

Fig. 4 shows the IRD(l_2,$\hat{\xi}$) diagram, which exchanges the robust scale estimator with the L-moment L-l2. The diagram is almost exactly the same, however it has one more advantage. The L-estimator is already scaled as $l_2 \in < 0, 1)$. The tail index is scaled as previously. The best PID obtains $d_{IRD(l_2,\hat{\xi})} = 0.268$ for the same parameters as previously. This observation is very important as it seems that the L-scale l_2 estimator fits our requirements.

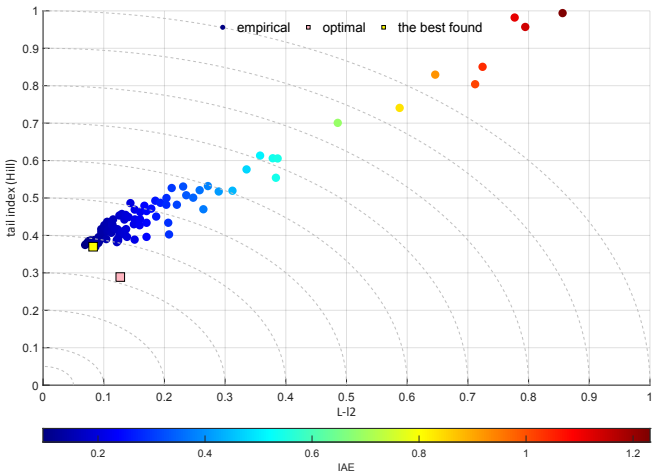

Fig. 6: IRD(l_2,$\hat{\xi}$) diagram for $G_1(s)$: pink square depicts good tuning, while yellow – the best found

Thus, further steps should investigate the possibility to exchange the tail index with other factors that are already scaled. There are two alternatives: the stability index α and the L-kurtosis. The is limited $\alpha \in \langle 0, 2 \rangle$ and therefore we may easily select the OY scaling to $y_{max} = 2$. Fig. 7 presents the respective diagram. This kind of plot is characterized with a different challenge: what is the best point. For sure, it's not the origin. Let's make a working hypothesis that it should

be an independent Gaussian noise [3], so we measure the distance to the point $[0;2]$. The best indicated controller gets $d_{IRD(l_2,\alpha)} = 0.054$ for $k_p = 0.05$ and $T_i = 0.20$.

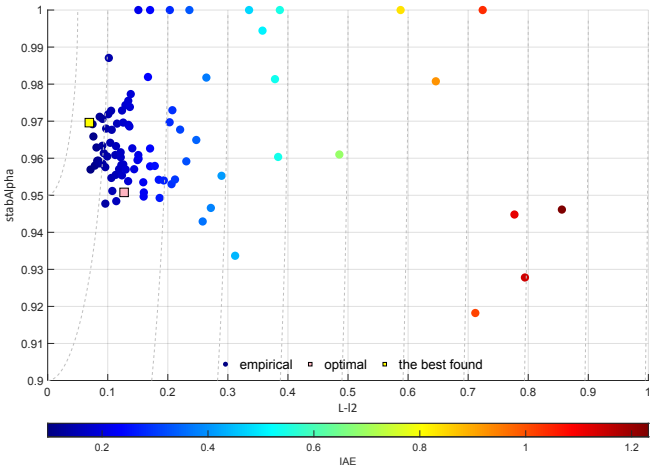

Fig. 7: IRD(l_2,α) diagram for $G_1(s)$: pink square depicts good tuning, while yellow – the best found

The last investigated variant of index ratio diagrams is the IRD(l_2,τ_4) shown in Fig. 8. This plot does not require any scaling as the L-kurtosis cannot exceed 1.0 and we assume that it should not get negative values. In this case similar discussion of the optimal point appears. Following previous assumption we select the point $[0;0.1226]$. As expected, this plot detects the same controller as previously with $d_{IRD(l_2,\tau_4)} = 0.051$.

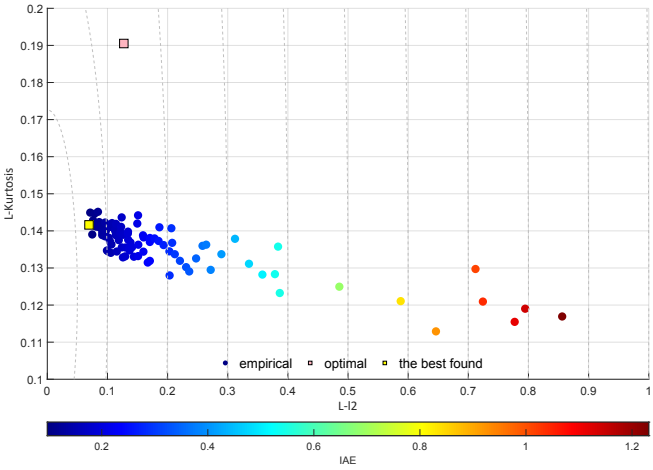

Fig. 8: IRD(l_2,τ_4) diagram for $G_1(s)$: pink square depicts good tuning, while yellow – the best found

Concluding, we get three options to be considered. The IRD(σ_R,$\hat{\xi}$) diagram requires relative scaling in both axes, while the IRD(l_2,$\hat{\xi}$) needs scaling only in OY. They both indicate the same solution. Thus, it's obvious to favor the second one. In the second group we have diagrams that do not require any relative decision about scaling (IRD(l_2,α) and IRD(l_2,τ_4)), but there is an assumption about the so called optimal zero point, which is not so obvious as it seems [27]. The comparison of the performance of the detected controllers is shown in Table I.

TABLE I: Performance of indicated controller for $G_1(s)$

	k_p	T_i	T_d	κ [%]	T_{set} [s]
IRD(σ_R,$\hat{\xi}$) IRD(l_2,$\hat{\xi}$)	0.55	3.2	0.9293	0.0	19.7
IRD(l_2,α) IRD(l_2,τ_4)	0.05	0.2	0.9293	32.8	38.5

The analysis of the above results suggest to use the IRD(l_2,$\hat{\xi}$) diagram as it requires the least relativity in the scaling selection and delivers reasonable results. The analysis of the consecutive two process aims at the validation of this hypothesis. Tables II and III present the analogous results for processes $G_4(s)$ and $G_5(s)$, respectively.

TABLE II: Performance of indicated controller for $G_4(s)$

	k_p	T_i	T_d	κ [%]	T_{set} [s]
IRD(σ_R,$\hat{\xi}$) IRD(l_2,α) IRD(l_2,τ_4)	0.2	0.1	0.2121	$\gg 100$	$\gg 1000$
IRD(l_2,$\hat{\xi}$)	0.2	1.1	0.2121	0.0	20.6

TABLE III: Performance of indicated controller for $G_5(s)$

	k_p	T_i	T_d	κ [%]	T_{set} [s]
IRD(σ_R,$\hat{\xi}$) IRD(l_2,$\hat{\xi}$)	0.02	0.05	0.0808	1.7	5.8
IRD(l_2,α) IRD(l_2,τ_4)	0.02	0.3	0.0808	0.0	56.4

We notice that the IRD(l_2,$\hat{\xi}$) in all cases allows to deliver reliable results. The following Figs. 9 and 10 show the respective plots for both transfer functions: $G_4(s)$ and $G_5(s)$.

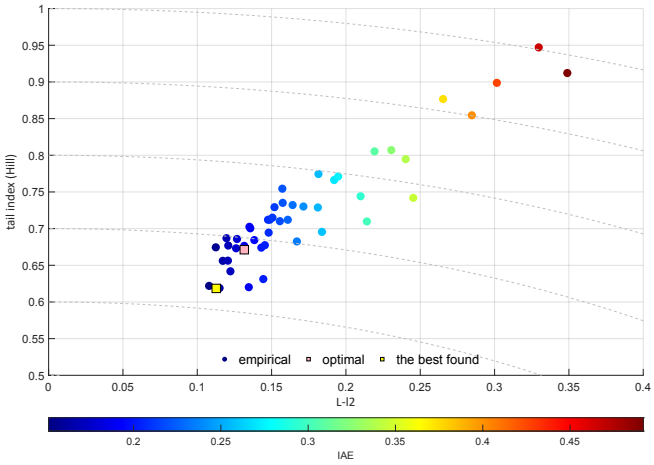

Fig. 9: IRD(l_2,$\hat{\xi}$) diagram for $G_4(s)$: pink square depicts good tuning, while yellow – the best found

Simulations give the possibility to change the tuning as we wish. We do not have to take care about potential poor behavior, that might deteriorate real process operation. In practice we do not have such comfort and we have may check only a few tuning sets. The IRD plot shows only single point.

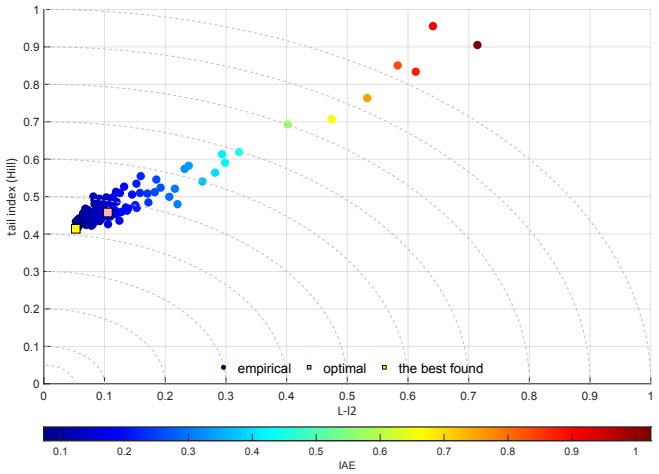

Fig. 10: IRD(l_2,$\hat{\xi}$) diagram for $G_5(s)$: pink square depicts good tuning, while yellow – the best found

Its position depends on the performance, but it is affected by the process itself. We cannot decide, which position in the diagram is better. It's relative.

However, it doesn't mean that the IRD has no practical value. We should extend horizons. We can add the time to the analysis or we can compare different loops looking for their similarities. These issues have been already investigated [28] in the practical sense.

IV. CONCLUSIONS AND FURTHER RESEARCH

This paper introduces the Index Ratio Diagrams into the control research and practice. It shows that proper selection of the diagrams allows to determine poor and good tuning. It is suggested to investigate further and validate the potential of the IRD(l_2,$\hat{\xi}$) diagram. It considers new CPA indicators as the L-variance l_2 and the tail index $\hat{\xi}$.

The simulation analysis shows the potential of the proposed approach. However, these initial results just only open new options. There is a need to investigate further the properties of the L-moments and tail index in the control engineering research context. Next, the aspect of the tail index scaling should be investigated.

The other types of the IRD diagrams should not be forgotten, as there is an open issue with the selection of the well-tuned point in case of the target L-Kurtosis and the stability index α. This paper shows that there is much to be done in this research especially in combining simulations with an engineering practice.

REFERENCES

[1] Bauer, M., Horch, A., Xie, L., Jelali, M. and Thornhill, N., The current state of control loop performance monitoring – A survey of application in industry, *Journal of Process Control*. vol. 38, 2016, pp. 1–10.

[2] Samad, T., A Survey on Industry Impact and Challenges Thereof [Technical Activities], *IEEE Control Systems Magazine*. vol. 37, no. 1, 2017, pp. 17–18.

[3] Domański, P.D., *Control Performance Assessment: Theoretical Analyses and Industrial Practice*. Springer International Publishing, Cham, Switzerland, 2020.

[4] Åström, K.J., A Survey on Industry Impact and Challenges Thereof [Technical Activities], *IBM Journal*. vol. 11, 1967, pp. 389–405.

[5] Spinner, T., Srinivasan, B. and Rengaswamy, R., Data-based automated diagnosis and iterative retuning of proportional-integral (PI) controllers, *Control Engineering Practice*. vol. 29, 2014, pp. 23–41.

[6] Kaczmarek, K. and Domański, P.D., Study on outlier robustness of minimum variance control performance assessment, *International Journal on Adaptive Control and Signal Processing*. vol. 35, no. 11, 2021, pp. 2175–2193.

[7] Veronesi, M. and Visioli, A., Performance Assessment and Retuning of PID Controllers for Load Disturbance Rejection, *IFAC Proceedings Volumes, 2nd IFAC Conference on Advances in PID Control*. vol. 45, no. 3, 2012, pp. 530–535.

[8] Knierim-Dietz, N., Hanel, L. and Lehner, J., *Definition and verification of the Control Loop Performance for Different Power Plant Types*, Technical Report, Institute of Combustion and Power Plant Technology, University of Stutgart, 2012.

[9] Chaber, P. and Domański, P.D., Control Assessment with Moment Ratio Diagrams, in *Advanced, Contemporary Control*, eds. Pawelczyk, M., Bismor, D. Ogonowski, S. and Kacprzyk, J., Springer Nature Switzerland, 2023, pp. 530–535.

[10] Hosking, J.R.M., L-Moments: Analysis and Estimation of Distributions Using Linear Combinations of Order Statistics, *Journal of the Royal Statistical Society. Series B (Methodological)*. vol. 52, 1990, pp. 105–124.

[11] Kaniuka, J.; Ostrysz, J.; Groszyk, M.; Bieniek, K.; Cyperski, S. and Domański, P.D., Study on Cost Estimation of the External Fleet Full Truckload Contracts, *Proceedings of the 20th International Conference on Informatics in Control, Automation and Robotics*. vol. 2, 2023, pp. 316–323.

[12] Qi, Y, On the tail index of a heavy tailed distribution, *Annals of the Institute of Statistical Mathematics*. vol. 62, 2010, pp. 277–298.

[13] Domański, P.D., Non-Gaussian properties of the real industrial control error in SISO loops, *Proceedings of the 19th International Conference on System Theory, Control and Computing*, 2015, pp. 877–882.

[14] Rousseeuw, P. J. and Leroy, A. M., *Robust Regression and Outlier Detection*. John Wiley & Sons, Inc., New York, NY, USA, 1987.

[15] Domański, P.D., Non-Gaussian properties of the real industrial control error in SISO loops, *International Journal of Automation and Computing*, vol. 17, no. 6, 2020, pp. 788–811.

[16] Peel, M., Wang, Q. and McMahon, T., The utility L-moment ratio diagrams for selecting a regional probability distribution, *Hydrological Sciences Journal*, vol. 46, 2001, pp. 147–155.

[17] Hosking, J.R.M., Moments or L-Moments? An Example Comparing Two Measures of Distributional Shape, *The American Statistician*. vol. 46, no. 3, 1992, pp. 186–189.

[18] Huber, P.J. and Ronchetti, E.M. *Robust Statistics, 2nd Edition*, New York: Wiley, 2009.

[19] Verboven, S. and Hubert, M. LIBRA: a Matlab library for robust analysis, *Chemometrics and Intelligent Laboratory Systems*. vol. 75, no. 2, 2005, pp. 127–136.

[20] Vargo, E., Pasupathy, R. and Leemis, L. oment-ratio diagrams for univariate distributions, *Journal of Quality Technology*. vol. 42, no. 3, 2010, pp. 1–11.

[21] Davis, R. and Resnick, S. Tail estimates motivated by extreme value theory, *The Annals of Statistics*. vol. 12, no. 4, 1984, pp. 1467–1487.

[22] Taleb, N.N. Statistical Consequences of Fat Tails: Real World Preasymptotics, Epistemology, and Applications, *arXiv:2001.10488*. rev.3, 2022.

[23] Fedotenkov, I. A Review of More than One Hundred Pareto-Tail Index Estimators, *Statistica*. vol. 80, no. 3, 2020, pp. 245–299.

[24] Hill, B.M. A simple general approach to inference about the tail of a distribution, *The Annals of Statistics*. vol. 3, no. 5, 1975, pp. 1163–1174.

[25] Huisman, R., Koedijk, K.G., Kool, C.J.M. and Palm, F. Tail-index estimates in small samples, *Journal of Business & Economic Statistics*. vol. 19, no. 2, 2001, pp. 208–216.

[26] Åström, K. J. and Hägglund, T., Benchmark Systems for PID Control, *IFAC Digital Control: Past, Present and Future of PlD Control*. 2000, pp. 165–166.

[27] Chaber, P. and Domański, P.D., Fractional control performance assessment of the nonlinear mechanical systems, in *Proc. of the Nonlinear Dynamics Conference NODYCON2023*, Rome, Italy, 2023.

[28] Domański, P. D., Jankowski, R., Dziuba, K. and Góra, R., Assessing Control Sustainability Using L-Moment Ratio Diagrams, *Electronics*. vol. 12, no. 11, 2023, 2377